Arteriosclerosis, Thrombosis, and Vascular Biology

TRANSLATIONAL SCIENCES

Identification of Celastrol as a Novel Therapeutic Agent for Pulmonary Arterial Hypertension and Right Ventricular Failure Through Suppression of Bsg (Basigin)/CyPA (Cyclophilin A)

Ryo Kurosawa, Kimio Satoh, Takashi Nakata, Tomohiko Shindo, Nobuhiro Kikuchi, Taijyu Satoh, Mohammad A.H. Siddique, Junichi Omura, Shinichiro Sunamura, Masamichi Nogi, Yutaro Takeuchi, Satoshi Miyata, Hiroaki Shimokawa

OBJECTIVE: Pulmonary arterial hypertension is characterized by abnormal proliferation of pulmonary artery smooth muscle cells and vascular remodeling, which leads to right ventricular (RV) failure. Bsg (Basigin) is a transmembrane glycoprotein that promotes myofibroblast differentiation, cell proliferation, and matrix metalloproteinase activation. CyPA (cyclophilin A) binds to its receptor Bsg and promotes pulmonary artery smooth muscle cell proliferation and inflammatory cell recruitment. We previously reported that Bsg promotes cardiac fibrosis and failure in the left ventricle in response to pressure-overload in mice. However, the roles of Bsg and CyPA in RV failure remain to be elucidated.

APPROACH AND RESULTS: First, we found that protein levels of Bsg and CyPA were upregulated in the heart of hypoxia-induced pulmonary hypertension (PH) in mice and monocrotaline-induced PH in rats. Furthermore, cardiomyocyte-specific Bsg-overexpressing mice showed exacerbated RV hypertrophy, fibrosis, and dysfunction compared with their littermates under chronic hypoxia and pulmonary artery banding. Treatment with celastrol, which we identified as a suppressor of Bsg and CyPA by drug screening, decreased proliferation, reactive oxygen species, and inflammatory cytokines in pulmonary artery smooth muscle cells. Furthermore, celastrol treatment ameliorated RV systolic pressure, hypertrophy, fibrosis, and dysfunction in hypoxia-induced PH in mice and SU5416/hypoxia-induced PH in rats with reduced Bsg, CyPA, and inflammatory cytokines in the hearts and lungs.

CONCLUSIONS: These results indicate that elevated Bsg in pressure-overloaded RV exacerbates RV dysfunction and that celastrol ameliorates RV dysfunction in PH model animals by suppressing Bsg and its ligand CyPA. Thus, celastrol can be a novel drug for PH and RV failure that targets Bsg and CyPA.

GRAPHIC ABSTRACT: A graphic abstract is available for this article.

Key Words: basigin ■ fibrosis ■ heart failure ■ hypertension, pulmonary ■ inflammation ■ mice

Downloaded from http://ahajournals.org by on March 22, 2021

Pulmonary arterial hypertension (PAH) is characterized by abnormal proliferation of pulmonary artery smooth muscle cells (PASMCs) and vascular remodeling, which leads to right ventricular (RV) failure and premature death.[1–6] However, all the drugs in clinical use for PAH are essentially pulmonary vasodilators.[2,7] Thus, it is important to develop novel drugs that possess different mechanisms of action.[8–12] Bsg (Basigin), also known as CD147 or extracellular matrix metalloproteinase inducer, is a transmembrane glycoprotein that interacts with MCT (monocarboxylate transporter) family of proteins, MCT1 and MCT4, integrin, caveolin-1, and cyclophilins. Bsg promotes cell survival, chemotaxis, and MMPs (matrix metalloproteinases) activity, leading to cancer metastasis,

Correspondence to: Kimio Satoh, MD, PhD, Department of Cardiovascular Medicine, Tohoku University Graduate School of Medicine, 1-1 Seiryo-machi, Aoba-ku, Sendai 980-8574, Japan. Email satoh-k@cardio.med.tohoku.ac.jp

This article was sent to William C. Sessa, Consulting Editor, for review by expert referees, editorial decision, and final disposition.

The Data Supplement is available with this article at https://www.ahajournals.org/doi/suppl/10.1161/ATVBAHA.120.315731.

For Sources of Funding and Disclosures, see page 1216.

© 2021 American Heart Association, Inc.

Arterioscler Thromb Vasc Biol is available at www.ahajournals.org/journal/atvb

Nonstandard Abbreviations and Acronyms

Bsg	basigin
Bsg-Tg	cardiomyocyte-specific Bsg-overexpressing
CyPA	cyclophilin A
ERK1/2	extracellular signal–regulated kinase 1/2
LV	left ventricle
MAPK	mitogen-activated protein kinase
MCT	monocarboxylate transporter
MMP	matrix metalloproteinase
NF-κB	nuclear factor-κb
NRCM	neonatal rat cardiomyocyte
PAB	pulmonary artery banding
PAH	pulmonary arterial hypertension
PASMC	pulmonary artery smooth muscle cell
PH	pulmonary hypertension
ROS	reactive oxygen species
RV	right ventricle
RVH	right ventricular hypertrophy
RVSP	right ventricular systolic pressure
sBsg	soluble Bsg

atherosclerosis, and left ventricular (LV) failure.[13–15] Also, Bsg is an essential receptor for CyPA (cyclophilin A) that binds to cyclosporine, an immunosuppressant.[13] Cyclophilins are members of the immunophilin family of peptidyl-prolyl cis-trans isomerases working as chaperones and mediators of protein folding.[16] The cyclosporine-CyPA complex inhibits a calcium/calmodulin-dependent phosphatase, calcineurin, leading to suppression of organ rejection.[16] Aside from their function as protein chaperones, cyclophilins also mediate chemotaxis of neutrophils, eosinophils, and T cells when secreted from cells in response to oxidative stress.[17,18] Moreover, secreted CyPA binds to Bsg in the plasma membrane, which induces proliferation and inflammatory cell recruitment, leading to atherosclerosis, cardiac hypertrophy, and pulmonary hypertension (PH).[14,19,20] We have previously reported that both Bsg and CyPA exacerbate PH in hypoxia-induced PH in mice and that high plasma CyPA levels were associated with poor outcome in patients with PAH.[14] Furthermore, we have also reported that Bsg promotes cardiac fibrosis and failure in LV in response to chronic pressure-overload in mice and that high plasma levels of both soluble form of Bsg (sBsg) and CyPA were associated with poor prognosis in patients with LV failure.[15,21,22] Also, *BSG rs8259* polymorphism was associated with Bsg expression and risk of chronic heart failure and acute coronary syndrome.[23,24] However, the roles of Bsg and CyPA in RV failure are still unknown.

We previously identified celastrol as a suppressor of Bsg and CyPA, which ameliorated LV failure in response to pressure-overload induced by transverse aortic constriction.[21] Celastrol is a quinone methide triterpene isolated from the root extracts of *Tripterygium wilfordii* plant, which is used in Chinese medicine to treat immunologic disorders, including rheumatoid arthritis.[25] There have been clinical trials using *Tripterygium wilfordii* for the treatment of Crohn's disease, psoriasis, rheumatoid arthritis, diabetes, and rejection after kidney transplantation, in which *Tripterygium wilfordii* had therapeutic effects for these diseases with relatively small side effects.[25] Celastrol, a main component of the root extracts of *Tripterygium wilfordii* , has antioxidant, anti-inflammatory, and anticancer properties, mainly attributed to its ability to inhibit NF-kB (nuclear factor-κB), a central player in inflammation and cancer.[25] Using a high-throughput screening system, we first discovered that celastrol effectively suppresses the expression of Bsg and CyPA in PASMCs and cardiac myocytes.[21] Also, it is reported that Bsg-cyclophilin interactions may be a good target for new anti-inflammatory therapeutics.[26,27]

Thus, in this study, we examined the role of Bsg in RV failure with cardiomyocyte-specific Bsg-overexpressing mice and the efficacy of celastrol as a suppressor of Bsg and CyPA for the treatment of PH and RV failure.

Highlights

- Protein levels of Bsg (basigin) and CyPA (cyclophilin A) in the right ventricles were elevated in animal models of pulmonary hypertension.
- Cardiomyocyte-specific Bsg-overexpressing mice showed exacerbated right ventricular function under chronic hypoxia and pulmonary artery banding.
- In vitro, celastrol treatment inhibited excessive proliferation, oxidative stress, and inflammation in pulmonary artery smooth muscle cells and oxidative stress and hypertrophy in cardiomyocytes, through suppression of Bsg and CyPA.
- Celastrol treatment ameliorated pulmonary hypertension and right ventricular failure in animal models of pulmonary hypertension and right ventricular pressure overload through suppression of Bsg and CyPA with reduced inflammation.

MATERIALS AND METHODS

Materials and Methods are available in the Data Supplement.

RESULTS

Protein Levels of Bsg and CyPA in the RVs of Animal Models of PH

Bsg is highly expressed in LV in patients with dilated cardiomyopathy, myocardial infarction, and inflammatory cardiomyopathy.[28–30] Additionally, plasma levels of sBsg and CyPA were higher in patients with LV failure

Downloaded from http://ahajournals.org by on March 22, 2021

compared with controls and were associated with poor prognosis.[15,21] Thus, we evaluated the protein levels of Bsg and CyPA in pressure-overloaded RV. Consistent with the previous reports, protein levels of Bsg and CyPA in RVs in animal models of PH were significantly higher compared with controls (Figure 1A and 1B).

RV Function in Cardiomyocyte-Specific Bsg-Overexpressing Mice

Next, to examine the role of Bsg in RV, we exposed cardiomyocyte-specific Bsg-overexpressing (Bsg-Tg) mice to chronic hypoxia (Figure 2A). During the 4 weeks of hypoxia, there was no difference in body weight between Bsg-Tg mice and controls (Figure 2B). We confirmed increased right ventricular systolic pressure (RVSP) and right ventricular hypertrophy (RVH) in mice under chronic hypoxia compared with normoxic mice (Figure 2C). Interestingly, Bsg-Tg mice showed exacerbated RVH compared with controls without a significant difference in RVSP under hypoxia (Figure 2C). In spite of equal pressure-overload (equal RVSP under hypoxia), Bsg-Tg mice showed exacerbated RV parameters (eg, RV wall thickness, RV diastolic diameter, RV fractional area change, tricuspid annular plane systolic excursion, RV myocardial performance index, and cardiac output) compared with controls (Figure 2D). In contrast, LV parameters did not show significant difference between Bsg-Tg mice and controls under either normoxia or hypoxia (Figure 2E). Additionally, Bsg-Tg mice showed hypoxia-induced increase in cardiac interstitial fibrosis compared with controls without significant morphological changes in pulmonary arteries (Figure 2F and 2G). These results suggest that Bsg overexpression in the heart deteriorated RV function under pressure-overload (elevated RVSP) induced by chronic hypoxia.

Furthermore, to evaluate the role of Bsg in RVs, we performed pulmonary artery banding (PAB) in Bsg-Tg and wild-type mice (Figure IA in the Data Supplement). During 3 weeks after PAB surgery, there was no significant difference in body weight between Bsg-Tg or control mice with or without PAB surgery (Figure IB in the Data Supplement). Also, there was no significant change in max velocity and pressure gradient in the main pulmonary arteries assessed by echocardiography between Bsg-Tg and wild-type mice (Figure IC in the Data Supplement). At the point of 3 weeks after PAB surgery, Bsg-Tg mice showed increased protein levels of Bsg in the RVs compared with wild-type mice, in which PAB increased protein levels of Bsg and CyPA in the RVs (Figure ID in the Data Supplement). Interestingly, Bsg-Tg mice showed exacerbated RV end-diastolic pressure

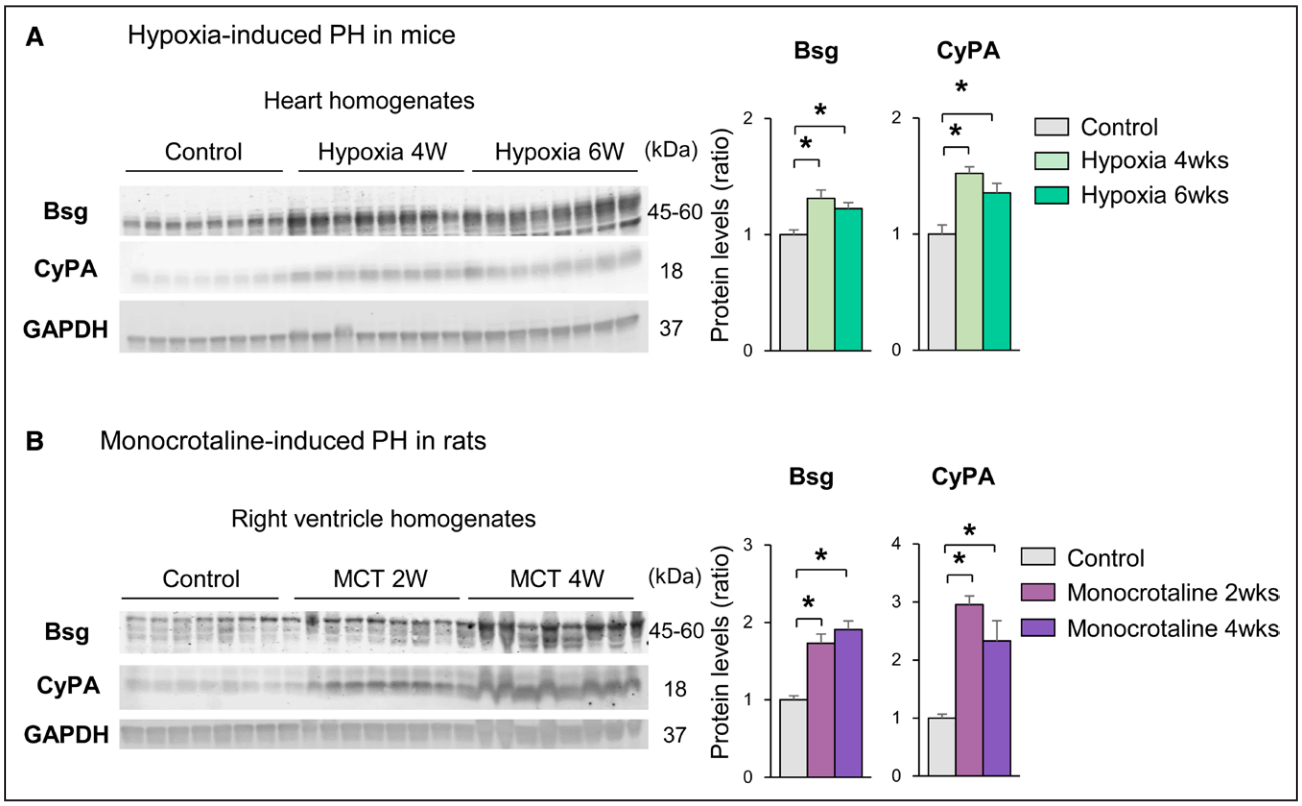

Figure 1. Pressure-overload upregulates protein levels of Bsg (basigin) and CyPA (cyclophilin A) in right ventricles.
A, Quantification of Bsg and CyPA in heart homogenates of control mice and hypoxia-induced pulmonary hypertension (PH) in mice exposed to hypoxia for 4 or 6 wk (n=8 each). **B**, Quantification of Bsg and CyPA in right ventricles of control rats and monocrotaline-induced PH in rats at 2 or 4 wks after monocrotaline (MCT) subcutaneous injection (n=8 each). Data represent the mean±SEM. *P<0.05. Comparisons of parameters were performed with 1-way ANOVA followed by Dunnett test for multiple comparisons.

Downloaded from http://ahajournals.org by on March 22, 2021

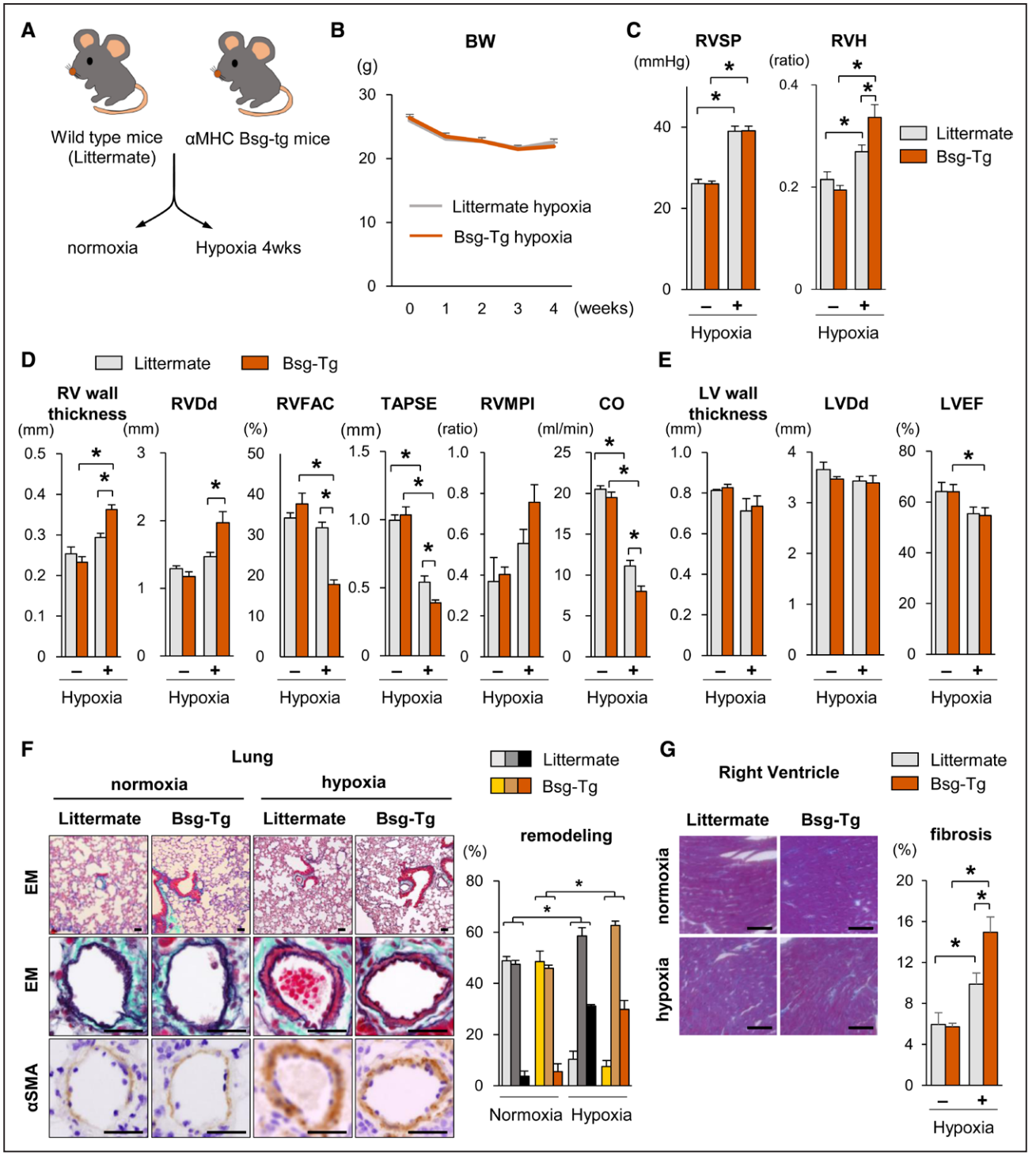

Figure 2. Right ventricular (RV) dysfunction in cardiomyocyte-specific Bsg (basigin)-overexpressing Mice.
A, Schematic protocols for chronic hypoxia (10% O_2) stimulation in cardiomyocyte-specific Bsg-overexpressing (Bsg-Tg) mice and controls. **B**, The time-course of body weight (BW) from the starting point of administration of celastrol or control vehicle under normoxia (21% O_2, n=8 each) or hypoxia (10% O_2, n=14 each) for 4 wk. **C**, Right ventricular systolic pressure (RVSP) and right ventricular hypertrophy (RVH) of Bsg-Tg mice and controls under normoxia or hypoxia (Bsg-Tg, n=16; control, n=4 each). RVH, the ratio of the right ventricle to the left ventricle plus septum (RV/LV+S). (**D**) Echocardiographic measurement of RV wall thickness, RV diastolic diameter (RVDd), RV fractional area change (RVFAC), tricuspid annular plane systolic excursion (TAPSE), RV myocardial performance index (RVMPI), and cardiac output (CO; Bsg-Tg, n=16; control, n=4 each). **E**, Echocardiographic measurement of left ventricular diastolic diameter (LVDd) and left ventricular ejection fraction (LVEF) (Bsg-Tg, n=16; control, n=4 each). **F**, Left, representative images of Elastica-Masson (EM) staining of distal pulmonary arteries (PAs) after chronic hypoxia. Right, quantitative analysis of remodeling in distal PA (Bsg-Tg, n=16; control, n=4 each). Scale bars, 25 μm. **G**, Left, representative images of EM staining of hearts after chronic hypoxia. Right, quantitative analysis of interstitial fibrotic area (Bsg-Tg, n=16; control, n=4 each). Scale bars, 25 μm. Data represent the mean±SEM. *P<0.05. Comparisons of parameters were performed with 2-way ANOVA, followed by Tukey honestly significant difference test for multiple comparisons.

Downloaded from http://ahajournals.org by on March 22, 2021

and RVH compared with wild-type mice without a significant difference in RVSP, in which PAB surgery increased RVSP, RV end-diastolic pressure, and RVH (Figure IE in the Data Supplement). Moreover, Bsg overexpression exacerbated fibrosis and cross-sectional area in RVs compared with wild-type mice (Figure IF and IG in the Data Supplement). In contrast, there was no change in LV function between Bsg-Tg and wild-type mice (Figure IH in the Data Supplement). However, Bsg-Tg significantly exacerbated RV parameters (eg, RV diastolic diameter, RV fractional area change, tricuspid annular plane systolic excursion, RV myocardial performance index, S wave, and cardiac output) worsened by PAB, compared with wild-type mice (Figure II in the Data Supplement). Moreover, Bsg-Tg mice showed upregulated mRNA expression of hypertrophic markers, such as *Nppa* and *Nppb* in the RVs compared with wild-type mice (Figure IJ in the Data Supplement). These results suggest that Bsg overexpression in the heart deteriorated RV function under pressure-overload induced by PAB.

Celastrol-Mediated Suppression of Bsg and CyPA

We performed a high-throughput screening and identified celastrol that reduced the expressions of both CyPA (*Ppia*) and Bsg (*Bsg*) expression from 3336 clinically used compounds and derivatives, in which 113 compounds inhibited proliferation of PASMCs (Figure 3A). Consistently, celastrol treatment suppressed mRNA expression of *Bsg* and *Ppia* (Peptidylprolyl isomerase A, also known as CyPA; Figure 3B) and protein levels of Bsg and CyPA (Figure 3C) in PAH-PASMCs (Table I in the Data Supplement). Here, it has been reported that celastrol has antioxidant, anti-inflammatory, and anticancer properties.[25] Indeed, celastrol treatment inhibited the excessive proliferation of PAH-PASMCs (Figure 3D), which have special characteristics in terms of proproliferative and antiapoptotic features in common with cancer cells.[31] While it has been reported that higher levels of cytosolic reactive oxygen species (ROS) are mechanistically involved in the proliferation of PAH-PASMCs,[5] celastrol attenuated cytosolic ROS levels in PAH-PASMCs (Figure 3E). Furthermore, celastrol treatment significantly reduced the levels of cytokines/chemokines and growth factors secreted from PAH-PASMCs (Figure 3F). Altogether, celastrol treatment decreased protein levels of Bsg and CyPA, inhibiting abnormal proliferation in PAH-PASMCs with reduced ROS and inflammation.

Then, we examined effect of celastrol on neonatal rat cardiomyocytes (NRCMs). As previously reported,[21] celastrol treatment suppressed mRNA expression of *Bsg* and *Ppia* (Figure IIA in the Data Supplement) and protein levels of Bsg and CyPA (Figure IIB in the Data Supplement) in NRCMs. Also, celastrol treatment significantly reduced the levels of various cytokines/chemokines and growth factors secreted from NRCMs (Figure IIC in the Data Supplement). Next, we treated NRCMs with the α1-adrenergic receptor agonist, phenylephrine, which recapitulates much of the intracellular signaling during pressure-overload.[32] Celastrol treatment did not reduce cell number (Figure IID in the Data Supplement) but attenuated cytosolic ROS levels (Figure IIE in the Data Supplement) in NRCMs. Importantly, celastrol treatment ameliorated phenylephrine-induced hypertrophy in NRCMs (Figure IIF in the Data Supplement). These results suggest that celastrol treatment suppresses Bsg and CyPA in NRCMs with reduced ROS, inflammation, and hypertrophy.

Furthermore, we examined direct effects of celastrol on cardiac fibroblasts. Consistently, celastrol treatment suppressed mRNA expression of *Bsg* and *Ppia* (Figure IIIA in the Data Supplement) and protein levels of Bsg and CyPA (Figure IIIB in the Data Supplement) in cardiac fibroblasts. Importantly, celastrol treatment attenuated proliferation (Figure IIIC in the Data Supplement) and cytosolic ROS levels (Figure IIID in the Data Supplement) in cardiac fibroblasts. Also, celastrol treatment significantly reduced the levels of cytokines/chemokines and growth factors secreted from cardiac fibroblasts (Figure IIIE in the Data Supplement). These results suggest that celastrol treatment directly suppresses Bsg and CyPA in cardiac fibroblasts with reduced proliferation, ROS, and inflammation.

Finally, we examined whether overexpression of Bsg by using a Bsg-encoding plasmid in RV-derived cardiomyocytes can affect RV-derived cardiac fibroblasts in vitro. First, we confirmed that Bsg plasmid upregulates protein levels and mRNA expression of Bsg in RV-derived cardiomyocytes (Figure IVA and IVB in the Data Supplement), leading to exacerbated oxidative stress and production of cytokines compared with control plasmid group (Figure IVC and IVD). Importantly, treatment with conditioned medium from cardiomyocytes with Bsg plasmid increased proliferation and ROS in RV-derived cardiac fibroblasts, compared with conditioned medium from cardiomyocytes with control plasmid group (Figure IVE and IVF). In the previous studies, it was reported that β-adrenergic receptor stimulation and oxidative stress upregulate Bsg expression in cardiomyocytes, which activates MAPKs (mitogen-activated protein kinases) and upregulates MMPs, leading to adverse remodeling.[33,34] Also, we previously showed that Bsg signaling stimulated by CyPA and mechanical stretch in cardiac fibroblasts activates Akt and ERK1/2 (extracellular signal–regulated kinase 1/2) and induces cell proliferation, oxidative stress, and inflammatory cytokines, resulting in MMPs activation.[15] We also showed that MMPs cleave membrane-bound Bsg and release soluble extracellular domain of Bsg (sBsg), which interacts with membrane-bound Bsg again in an autocrine/paracrine manner.[15] In the present study, we showed that Bsg overexpression in

Downloaded from http://ahajournals.org by on March 22, 2021

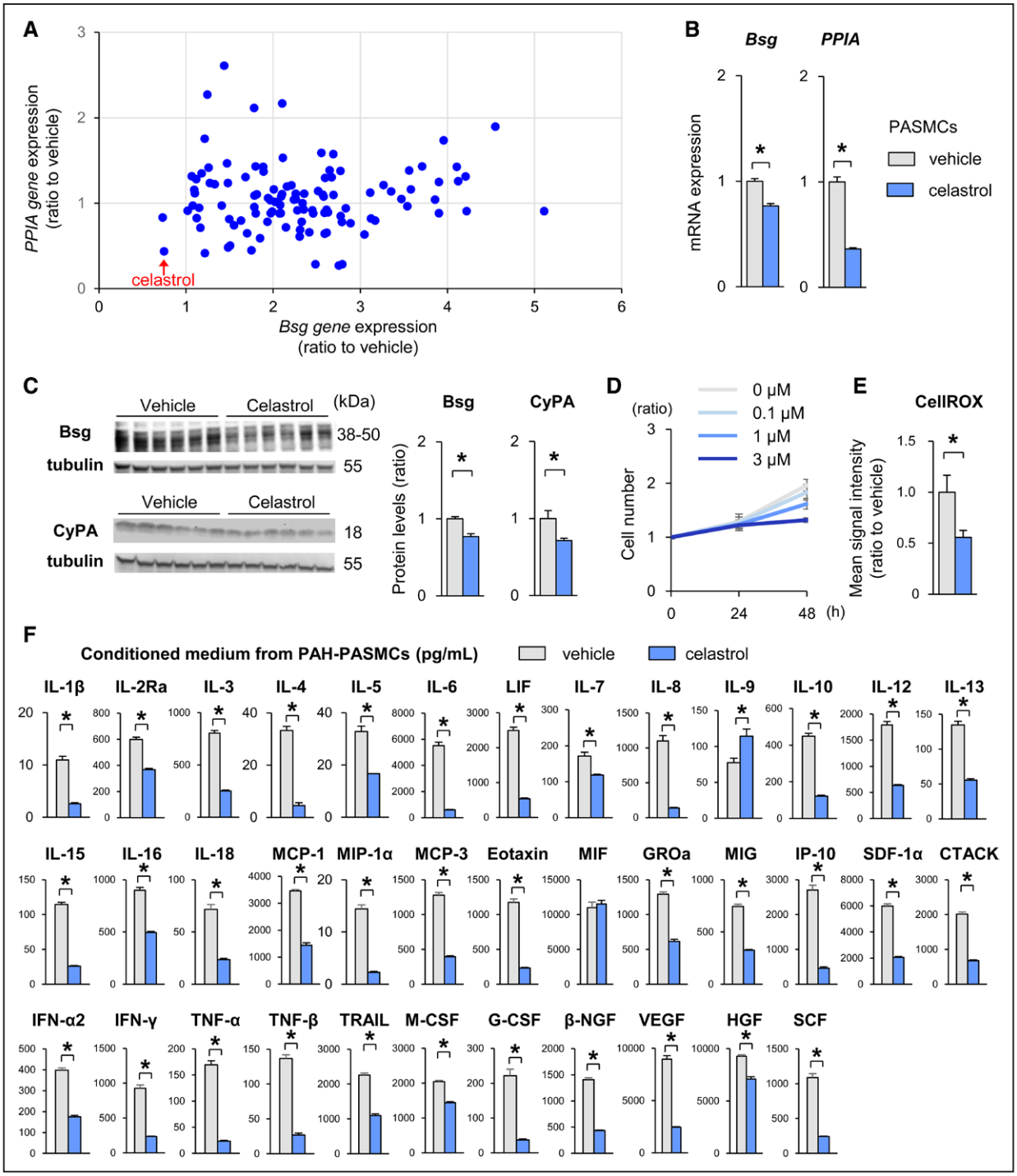

Figure 3. Celastrol-mediated suppression of Bsg (basigin) and CyPA (cyclophilin A).
A, RT-PCR analysis of *Ppia* (CyPA) and human *Bsg* (Bsg) gene expression after the treatment with 113 compounds that effectively suppress pulmonary artery smooth muscle cell (PASMC) proliferation in 3336 compounds in PASMCs from patients with pulmonary arterial hypertension (PAH). **B**, RT-PCR analysis of *Bsg* and *Ppia* mRNA in PAH-PASMCs after the treatment with celastrol 1 μmol/L or vehicle for 24 h (n=6). **C**, Quantification of Bsg and CyPA in PAH-PASMCs after the treatment with celastrol or vehicle for 24 h (n=6). **D**, MTT assay, in which cell viability was measured at 0, 24, 48 h after treatment with different concentrations (0, 0.1, 1, and 3 μmol/L) of celastrol (n=8 each) in PAH-PASMCs. **E**, Quantification of CellROX fluorescence intensity in PAH-PASMCs after the treatment with celastrol or vehicle for 24 h (n=8 each). **F**, Levels of cytokines/chemokines and growth factors in conditioned medium of PAH-PASMCs after the treatment with celastrol 3 μmol/L or vehicle for 24 h (n=6 each). Data represent the mean±SEM. *P<0.05. Comparisons of parameters were performed with unpaired Student t test. CTACK indicates cutaneous T-cell-attracting chemokine; G-CSF, granulocyte-colony stimulating factor; GRO, growth-regulated oncogenes; HGF, hepatocyte growth factor; IFN, interferon; IL, interleukin; IP, interferon γ-induced protein; M-CSF, macrophage colony-stimulating factor; MCP, monocyte chemotactic protein 1; MIF, macrophage migration inhibitory factor; MIG, monokine induced by gamma interferon; MIP, macrophage inflammatory protein; MTT, 3-(4,5-dimethylthial-2-yl)-2,5-diphenyltetrazalium bromide; NGF, nerve growth factor; SCF, stem cell factor; SD, stromal cell-derived factor; TNF, tumor necrosis factor; TRAIL, TNF-related apoptosis-inducing ligand; and VEGF, vascular endothelial growth factor.

Downloaded from http://ahajournals.org by on March 22, 2021

cardiomyocytes increase ROS and cytokines, affecting cardiac fibroblasts in a paracrine manner through sBsg (Figure IVG in the Data Supplement).

Celastrol Ameliorates Hypoxia-Induced PH in Mice

We have previously reported that both Bsg and CyPA exacerbates hypoxia-induced PH in mice and that high plasma CyPA levels were associated with poor outcome in patients with PAH.[14] In this study, we found that elevation of RVSP (pressure-overload in RVs) upregulated Bsg and CyPA in RVs, in which Bsg overexpression promoted RV dysfunction. Thus, we hypothesized that celastrol treatment would ameliorate PH and RV failure through inhibition of Bsg and CyPA (Figure 4A). Celastrol treatment significantly reduced body weight, which is consistent with the previous report (Figure 4B).[35] Moreover, celastrol treatment reduced mRNA expression of *Bsg* and *Ppia* (Figure 4C) and protein levels of Bsg and CyPA (Figure 4D) in the lungs compared with vehicle. Furthermore, celastrol treatment reduced phosphorylation of ERK (extracellular signal-regulated kinase; Thr202/Tyr204) and AKT (Ser473) in the lungs (Figure 4D). Importantly, celastrol treatment ameliorated hypoxia-induced PH assessed by RVSP, RVH, and pulmonary arterial remodeling (Figure 4E and 4F). Finally, cytokine/chemokines assay showed that celastrol treatment significantly reduced IL-1α and IL-2 in the lungs (Figure 4G and Figure VA in the Data Supplement).

Celastrol Ameliorates SU5416/Hypoxia-Induced PH in Rats

To further evaluate the therapeutic potential of celastrol for PAH, we used SU5416/hypoxia-induced PH model in rats, in which rats were exposed to chronic hypoxia for 21 days in combination with injection of SU5416 (Sugen/hypoxia model; Figure 5A). In this model, we started celastrol treatment after the establishment of PH (treatment protocol). Consistent with the previous study,[35] daily administration of celastrol for 14 days reduced body weight compared with vehicle controls (Figure VIA in the Data Supplement). Celastrol treatment reduced protein levels of Bsg in the lungs compared with vehicle controls (Figure 5B). Moreover, celastrol treatment significantly ameliorated PH, assessed by RVSP and RVH (Figure 5C) and suppressed muscularization of distal pulmonary arteries (Figure 5D) compared with controls. Cytokine/chemokine assay showed reduced protein levels of inflammatory cytokines (eg, IL-1α) in the lungs by celastrol treatment (Figure 5E). We further analyzed celastrol-mediated changes in RV morphology and function in SU5416/hypoxia-induced PH model in rats. Again, celastrol treatment reduced protein levels of Bsg and CyPA in RVs compared with controls, although they were not significantly elevated in the SU5416/ hypoxia vehicle group compared with the control group (Figure 6A). Additionally, celastrol treatment significantly suppressed RV fibrosis compared with controls (Figure 6B). In contrast, there was no change in LV morphology and function between celastrol and vehicle groups (Figure 6C). However, celastrol treatment significantly ameliorated RV parameters (eg, RV diastolic diameter, RV fractional area change, tricuspid annular plane systolic excursion, PAAT, and cardiac output) compared with controls (Figure 6D). Consistently, celastrol treatment improved exercise capacity evaluated by treadmill walking distance, compared with controls (Figure 6E). Cytokine/chemokine assay showed celastrol-mediated reduction of inflammatory cytokines (eg, Il-2, IL-4, and IFN-γ) in the hearts compared with controls (Figure 6F). Finally, celastrol treatment reduced plasma levels of cytokines/chemokines and growth factors compared with controls (Figure VIB in the Data Supplement). These results suggest that celastrol suppresses Bsg and CyPA with less inflammation in the lungs and RVs, ameliorating PH and RV failure in 2 PH animal models.

Celastrol Ameliorates PAB-Induced RV Failure in Mice

To evaluate the effect of celastrol on RV itself, we treated mice with PAB with celastrol for 21 days after PAB (Figure VIIA in the Data Supplement). Consistent with the previous study,[35] daily administration of celastrol for 21 days reduced body weight compared with vehicle controls in both groups of PAB and control mice (Figure VIIB in the Data Supplement). There was no significant change in max velocity or pressure gradient in the main pulmonary arteries assessed by echocardiography between the celastrol and the vehicle groups (Figure VIIC in the Data Supplement). Celastrol treatment significantly reduced protein levels of Bsg and CyPA in the RVs compared with vehicle controls (Figure VIID in the Data Supplement). Moreover, celastrol treatment significantly ameliorated RVH without a significant difference in RVSP (Figure VIIE in the Data Supplement) and reduced fibrosis and cross-sectional area in RVs compared with controls (Figure VIIF and VIIG in the Data Supplement). In contrast, there was no change in LV function between the 2 groups (Figure VIIH in the Data Supplement). However, celastrol treatment significantly ameliorated RV parameters (eg, RV diastolic diameter, RV fractional area change, tricuspid annular plane systolic excursion, RV myocardial performance index, S wave, and cardiac output) compared with controls (Figure VIII in the in the Data Supplement). Moreover, celastrol treatment tended to reduce mRNA expression of hypertrophic markers, such as *Nppa* and *Nppb* (Figure VIIJ in the in the Data Supplement) in the RVs compared with vehicle. These results suggest that celastrol suppresses Bsg and CyPA in the RVs and ameliorates RV failure itself under

Downloaded from http://ahajournals.org by on March 22, 2021

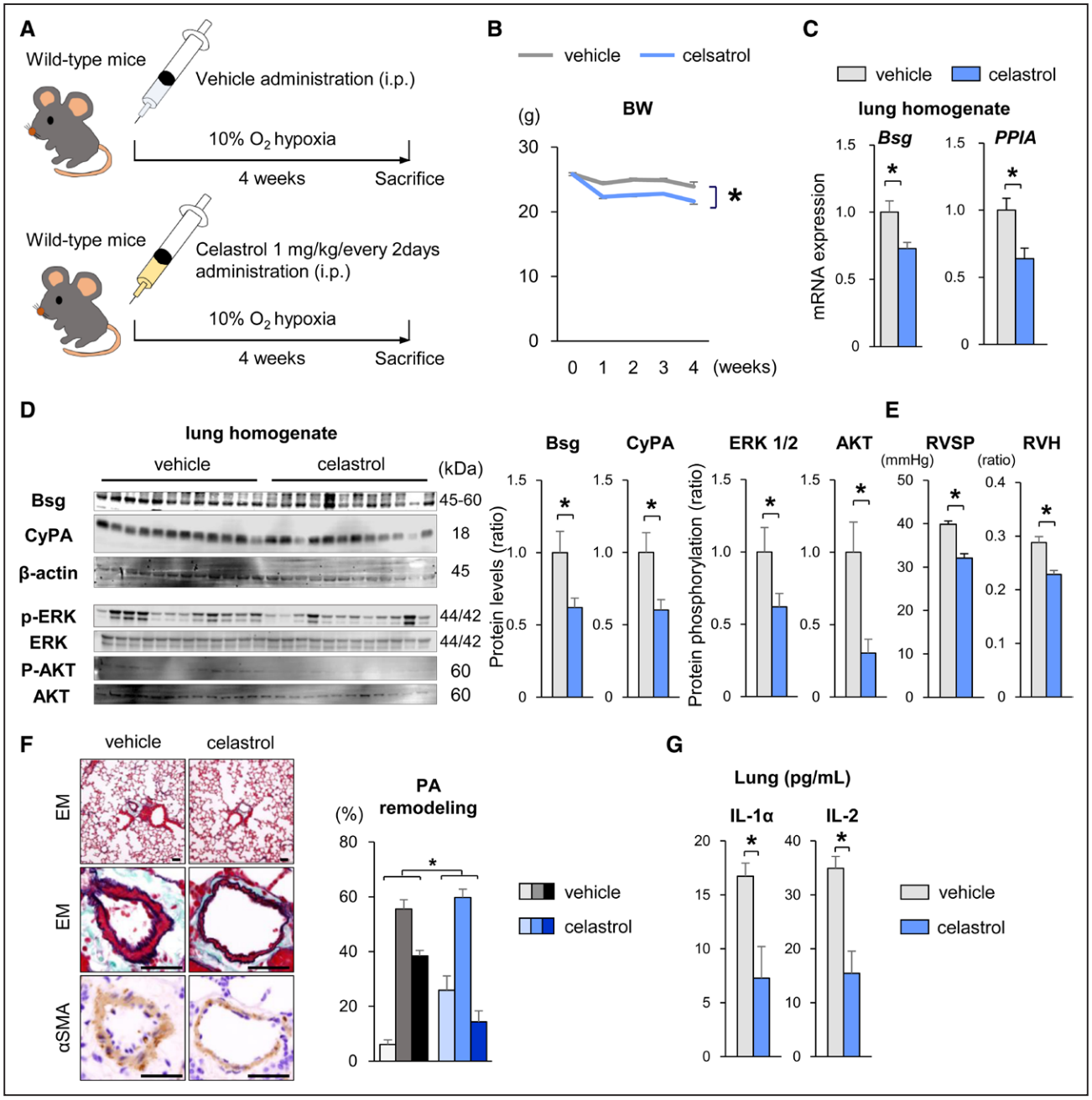

Figure 4. Celastrol ameliorates hypoxia-induced pulmonary hypertension in mice.
A, Schematic protocols for celastrol administration to hypoxia-induced pulmonary hypertension (PH) in wild-type mice, in which 1 mg/kg per 48 h celastrol or vehicle was intraperitoneally injected during the 4 wk of hypoxic exposure (10% O_2). **B**, The time-course of body weight (BW) from the starting point of administration of celastrol or vehicle under hypoxia (10% O_2, n=15 each) for 4 wk. **C**, RT-PCR analysis of Bsg (*Bsg*) and CyPA (cyclophilin A; *Ppia*) mRNA in lung homogenates after the treatment with celastrol or vehicle for 4 wks under hypoxia (n=12). **D**, Quantification of basigin (Bsg), CyPA, phosphorylated ERK (extracellular signal-regulated kinase) (Thr202/Tyr204), total ERK, phosphorylated AKT (Ser473), and total AKT in lung homogenates after the treatment with celastrol or vehicle for 4 wk under hypoxia (n=12). **E**, Right ventricular systolic pressure (RVSP) and right ventricular hypertrophy (RVH) in wild-type mice after the treatment with celastrol or vehicle under hypoxia (10% O_2, n=15) for 4 wk. RVH, the ratio of the right ventricle to the left ventricle plus septum (RV/LV+S). **F**, Muscularization of the distal pulmonary arteries (PAs) with a diameter of 20 to 70 μm after the treatment with celastrol or vehicle under hypoxia (n=15 each). N, nonmuscularized vessels; P, partially muscularized vessels; F, fully muscularized vessels. Scale bar, 25 μm. **G**, Levels of cytokines/chemokines and growth factors in lung homogenates of hypoxia-induced PH in mice after the treatment with celastrol or vehicle for 4 wk (n=4). Data represent the mean±SEM. *P<0.05. Comparisons of parameters were performed with unpaired Student *t* test. αSMA indicates α-smooth muscle actin; and IL-1α, interferon-1α.

pressure overload. In summary, celastrol ameliorates both PA remodeling and RV failure through suppression of Bsg and CyPA, reducing oxidative stress, inflammation, and abnormal proliferation in PASMCs, and oxidative stress and hypertrophy in cardiomyocytes (Figure VIIIA in the Data Supplement).

Downloaded from http://ahajournals.org by on March 22, 2021

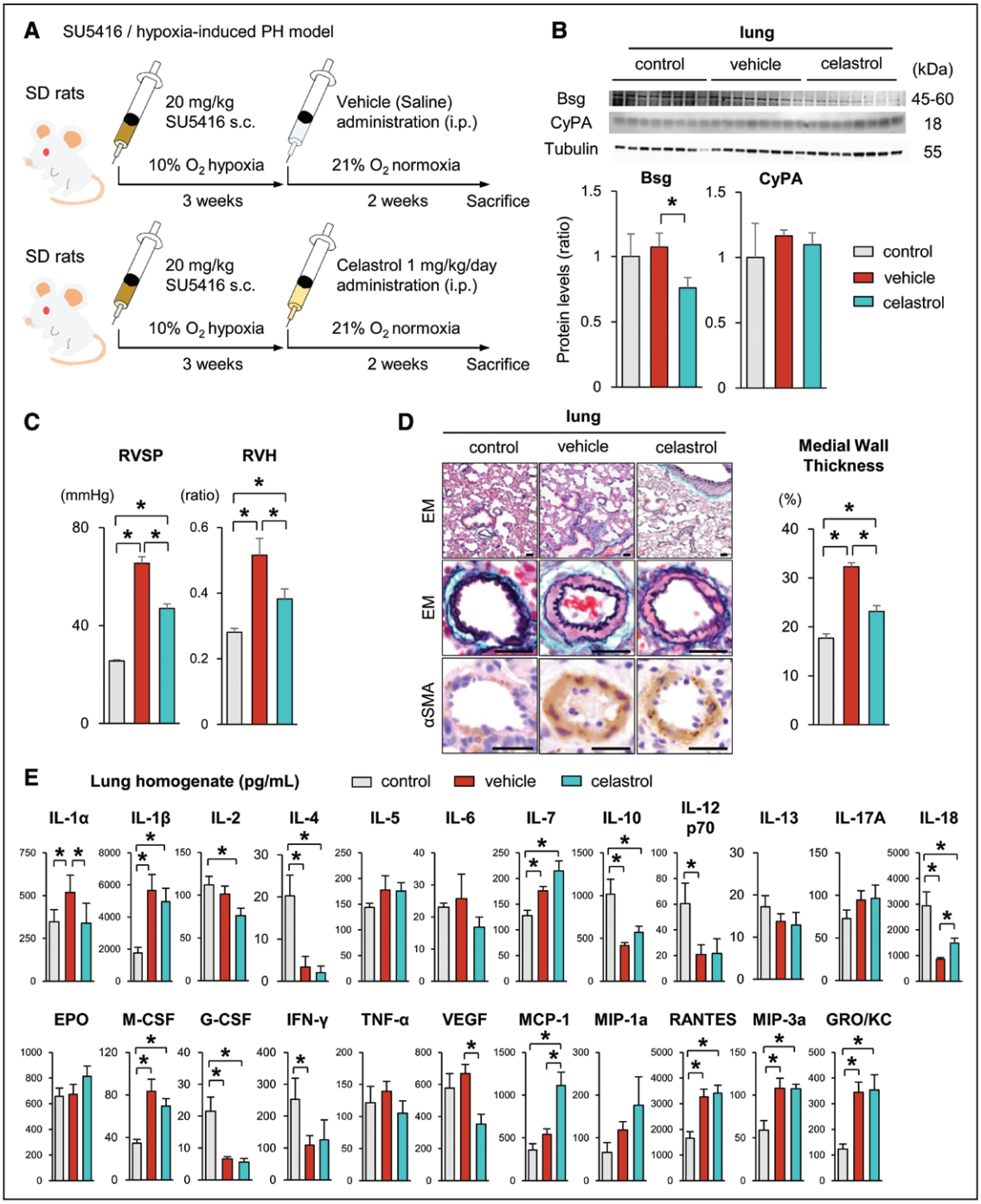

Figure 5. Celastrol ameliorates SU5416/ hypoxia-induced pulmonary hypertension in rats.
A, Schematic protocols for celastrol administration to SU5416/hypoxia-induced pulmonary hypertension (PH) in rats, in which rats were exposed to chronic hypoxia (10% O_2) for 3 wk in combination with the VEGF receptor blocker SU5416 (20 mg/kg, subcutaneous injection) followed by daily administration of 1 mg/kg celastrol or vehicle by intraperitoneal injection for 2 wk. **B**, Quantification of Bsg (basigin) and CyPA (cyclophilin A) in lung homogenates after the treatment with celastrol or vehicle (n=8 each). **C**, Right ventricular systolic pressure (RVSP) and right ventricular hypertrophy (RVH) in SU5416/hypoxia-induced PH in rats after the treatment with celastrol or vehicle (n=12 each). RVH, the ratio of the right ventricle to the left ventricle plus septum (RV/LV+S). **D**, Left, representative images of Elastica-Masson (EM) staining and α-SMA (α-smooth muscle actin) staining of distal pulmonary arteries of SU5416/hypoxia-induced PH in rats after the treatment with celastrol or vehicle. Scale bar, 25 μm. Right, medial wall thickness (MWT) of the distal pulmonary arteries with a diameter of 50 to 100 μm of SU5416/hypoxia-induced PH in rats after the treatment with celastrol or vehicle (n=12 each). **E**, Levels of cytokines/chemokines and growth factors in lung homogenates of SU5416/hypoxia-induced PH in mice after the treatment with celastrol or vehicle for 4 wk (n=8). Data represent the mean±SEM. *P<0.05. Comparisons of parameters were performed with 1-way ANOVA followed by Dunnett test for multiple comparisons. EPO indicates erythropoietin; G-CSF, granulocyte colony-stimulating factor; GRO/KC, growth-related oncogene/keratinocyte-derived chemokines; IFN-γ, interferon-γ; M-CSF, macrophage colony-stimulating factor; RANTES, regulated on activation, normal T-cell expressed and secreted; TNF-α, tumor necrosis factor-α; and VEGF, vascular endothelial growth factor.

Downloaded from http://ahajournals.org by on March 22, 2021

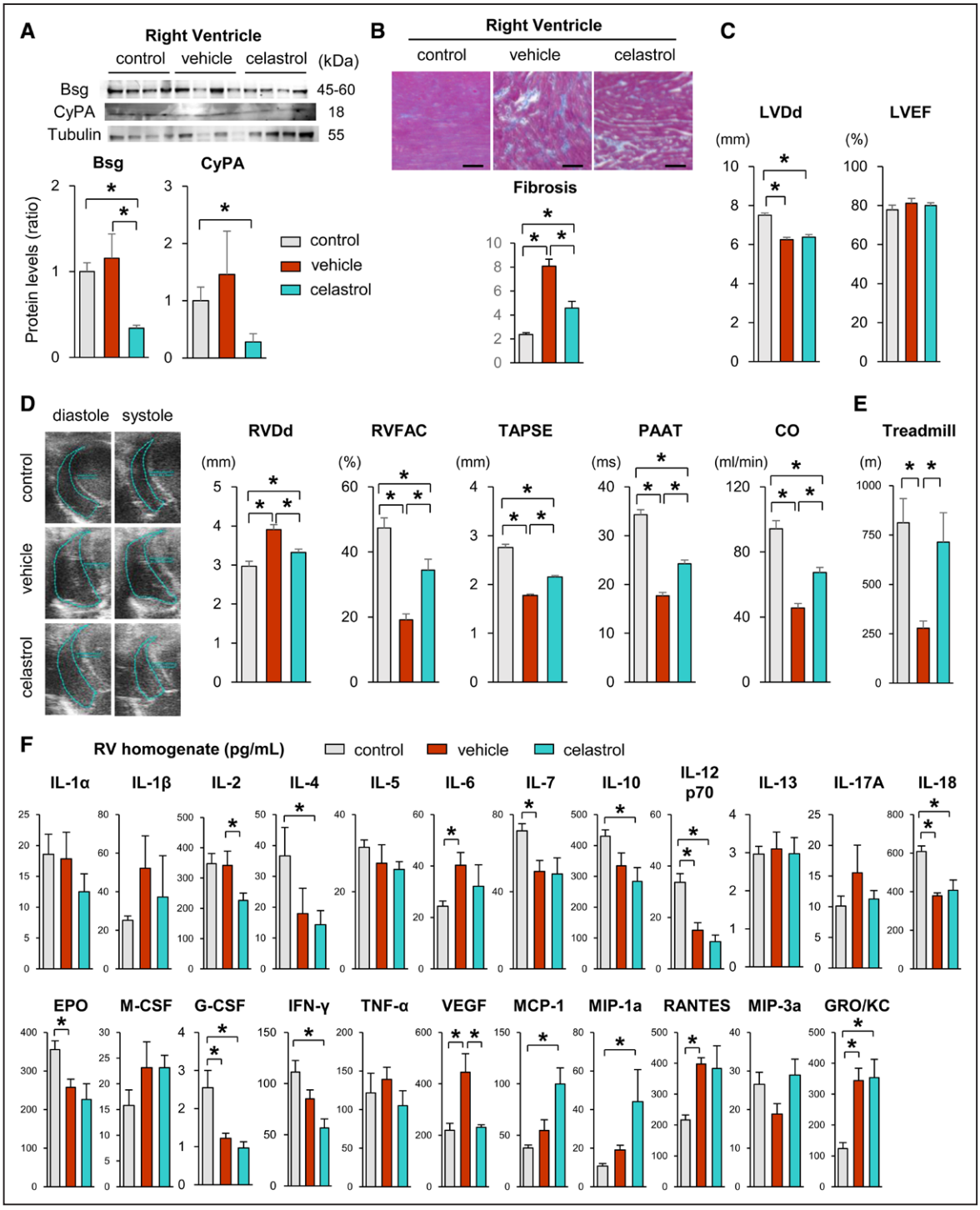

Figure 6. Celastrol ameliorates right ventricular dysfunction.

A, Quantification of Bsg (basigin) and CyPA (cyclophilin A) in right ventricular (RV) homogenates after the treatment with celastrol or vehicle (n=4). **B**, Up, representative pictures of Elastica-Masson (EM) staining of distal pulmonary arteries of SU5416/hypoxia-induced PH in rats after the treatment with celastrol or vehicle. Scale bar, 50 μm. Down, quantitative analysis of interstitial fibrotic area in RV of SU5416/hypoxia-induced PH in rats after the treatment with celastrol or vehicle (n=12 each). **C**, Echocardiographic measurement of left ventricular diastolic diameter (LVDd) and left ventricular ejection fraction (LVEF) (n=12 each). **D**, Left, representative echocardiographic images. Right, echocardiographic measurement of RV diastolic diameter (RVDd), RV fractional area change (RVFAC), tricuspid annular plane systolic excursion (TAPSE), pulmonary artery acceleration time (PAAT), and cardiac output (CO) (n=12 each). **E**, Walking distance assessed by treadmill test (n=12 each). **F**, Levels of cytokines/chemokines and growth factors in RV homogenates of SU5416/hypoxia-induced PH in rats after the treatment with celastrol or vehicle (n=4). Data represent the mean±SEM. **P*<0.05. Comparisons of parameters were performed with 1-way ANOVA followed by Dunnett test for multiple comparisons. EPO indicates erythropoietin; G-CSF, granulocyte colony-stimulating factor; IFN-γ, interferon-γ; M-CSF, macrophage colony-stimulating factor; MCP-1, monocyte chemotactic protein-1; MIP, macrophage inflammatory protein; RANTES, regulated on activation, normal T-cell expressed and secreted; TNF-α, tumor necrosis factor-α; and VEGF, vascular endothelial growth factor.

Downloaded from http://ahajournals.org by on March 22, 2021

DISCUSSION

In this study, we demonstrated that celastrol suppresses protein levels of Bsg and CyPA with reduced proliferation, oxidative stress, and inflammation, which ameliorates PH and RV function in animal models of PH. These concepts are based on the following findings; (1) the protein levels of Bsg and CyPA in RVs were elevated in animal models of PH, (2) cardiomyocyte- specific Bsg-overexpressing (Bsg-Tg) mice showed exacerbated RV dysfunction under chronic hypoxia, (3) celastrol inhibited proliferation, oxidative stress, and inflammation through suppression of Bsg and CyPA in PASMCs, (4) celastrol ameliorates hypoxia-induced PH in mice, and (5) celastrol ameliorates SU5416/hypoxia-induced PH and RV failure in rats through suppression of Bsg and CyPA with reduced inflammation.

Cardiomyocyte-Derived Bsg Induces Fibrosis in a Paracrine Manner

In the previous study, we demonstrated that severe left ventricular (LV) fibrosis developed in Bsg-Tg mice after transverse aortic constriction.[15] In addition, it has been reported that cardiomyocyte-derived Bsg induces MMPs and activates them by oxidative stress and β-adrenergic stimuli.[34] Also, membrane-bound Bsg can undergo proteolytic processing by MMPs to yield a sBsg, which interacts with membrane-bound Bsg on adjacent cardiac fibroblasts to further stimulate the production of MMPs and additional Bsg.[36] These findings indicate that overexpression of cardiomyocyte-specific Bsg leads to pressure overload–induced LV fibrosis and failure by activating MMPs with additional effects on cardiac fibroblasts in a paracrine manner. Furthermore, it has been reported that the role of MMPs in the right ventricle (RV) is important for remodeling followed by RV failure.[37] Importantly, treatment with cyclosporine A (CyPA inhibitor) or anti-Bsg antibody attenuated RV dysfunction induced by acute pulmonary embolism in rats, reducing activities of MMP-2 and MMP-9.[38] In the present study, treatment with conditioned medium from cardiomyocytes with Bsg plasmid increased proliferation and ROS in RV-derived cardiac fibroblasts, compared with conditioned medium from cardiomyocytes with control plasmid group. Taken together, these results suggest that Bsg overexpression in cardiomyocytes can affect cardiac fibroblasts in a paracrine manner, leading to fibrosis in the RVs of Bsg-Tg mice under pressure overload.

Bsg and CyPA Deteriorates RV Function

Protein levels of Bsg and CyPA in RVs were significantly elevated in animal models of PH. Additionally, Bsg overexpression in the heart promoted RV dysfunction under chronic hypoxia. Indeed, we previously showed that Bsg promotes cardiac fibrosis and failure in LVs in response to chronic pressure-overload in mice, in which Bsg is stimulated by CyPA, angiotensin II, mechanical stretch, and sBsg itself.[15] Stimulated Bsg activates Akt and ERK, inducing proliferation, oxidative stress, inflammation, and MMP activation with increased secretion of inflammatory cytokines and sBsg in fibroblasts, which leads to cardiac hypertrophy and fibrosis.[15] Also, it is reported that cardiac myocytes can increase the secretion of CyPA and expression of Bsg in response to hypoxia in vitro or ischemia in vivo to initiate prosurvival signaling in an autocrine fashion.[39] Thus, we think that PH (elevation of RVSP) induces Bsg and CyPA in pressure-overloaded RVs, increasing secretion of sBsg, CyPA, and inflammatory cytokines. These findings suggest that Bsg and CyPA play a crucial role in the development of RV failure under pressure-overload.

Celastrol As a Suppressor of Bsg and CyPA

Since agents targeting either Bsg or CyPA activity showed significant anti-inflammatory effects in various animal models, Bsg-CyPA interactions may be a good target for new anti-inflammatory therapeutics.[26,27] For indirect Bsg inhibition, berberine, resveratrol, and curcumin have been reported to inhibit Bsg expression through regulation of mitogen-activated protein kinase and ROS.[40–42] Inhibition of Bsg using anti-Bsg monoclonal antibody provided a >50% reduction of inflammation in mouse models of acute lung inflammation, asthma, and rheumatoid arthritis.[43] ABX-CBL is a murine IgM monoclonal antibody against the Bsg antigen, and a phase 2/3 multicenter randomized clinical trial showed effectiveness of ABX-CBL on graft-versus-host disease therapy.[44] Antagonistic peptides derived from extracellular domains of Bsg[45] or RNAi approach[46] are also attractive, but there is no report in vivo. Another arm of the Bsg-CyPA axis is cyclophilin-targeting drugs, and cyclosporine and FK-506 have been used for many years as immunosuppressors. However, immunosuppressive activity would cause an unwanted complication in the clinical use of these drugs as anti-inflammatory agents. Nonimmunosuppressive cyclosporine derivative, NIM811, exerted a potent anti-inflammatory activity, comparable to that of unmodified cyclosporine, in a mouse model of acute lung inflammation.[47] However, any of these therapeutics awaits further studies for clinical applications.

We previously identified celastrol as a suppressor of Bsg and CyPA, which reduced expression of Bsg and CyPA in PASMCs and cardiomyocytes, ameliorating LV failure and postcapillary PH in response to pressure-overload.[21] In the present study, we demonstrated that celastrol suppresses levels of Bsg, CyPA, and inflammation in these 3 cell types including PASMCs, cardiac fibroblasts, and cardiomyocytes. Many previous studies about celastrol revealed that therapeutic properties of celastrol are in inflammatory diseases, including rheumatoid arthritis, systemic lupus erythematosus, inflammatory bowel diseases, osteoarthritis, and allergy, as well as in cancer, neurodegenerative disorders, diabetes, obesity, atherosclerosis,

Downloaded from http://ahajournals.org by on March 22, 2021

and hearing loss.[25] Accumulating evidence indicates that the anti-inflammatory, anticancer properties of celastrol can be mainly attributed to its ability to inhibit NF-κB, a central player in inflammation and cancer, because inhibition of NF-κB reduces proinflammatory cytokine production,[48] MMP-2, MMP-9,[49] and ROS.[50] Here, celastrol is a main component of the root extracts of *Tripterygium wilfordii* plant, which is used in Chinese medicine to treat immunologic disorders, including rheumatoid arthritis, evidenced by many clinical trials.[25] Therefore, we think that celastrol has hopeful properties and could be a safe drug for the clinical use in the future.

In the present study, we found that celastrol reduces inflammatory cytokines and ROS levels via suppression of Bsg and CyPA in vitro and in vivo. Also, many studies showed that Bsg promotes CyPA-induced inflammation via mitogen-activated protein kinases and the NF-kB signaling pathway.[51,52] Therefore, these facts may imply that one of the main mechanisms of celastrol is inhibition of Bsg and CyPA, which reduces NF-κB, inflammatory cytokines, and ROS levels.

Study Limitations

There are some limitations to the present study. First, we found that celastrol treatment ameliorated RV dysfunction induced by pressure-overload, but it may be partially due to the reduced RVSP by direct effects on PASMCs. Second, we were unable to clearly show that celastrol ameliorates PH completely through suppression of Bsg and CyPA because it is technically difficult to show that overexpression of Bsg or CyPA cancels the effect of celastrol.

Clinical Implications and Conclusions

We found that protein levels of Bsg and CyPA in RVs were elevated in animal models of PH, which exacerbates pressure-overloaded RV dysfunction. Furthermore, celastrol, as a suppressor of Bsg and CyPA, successfully ameliorated PH and RV function in hypoxia-induced PH in mice and SU5416/hypoxia-induced PH in rats. In conclusion, celastrol could be a promising drug that targets Bsg and CyPA for the treatment of patients with PAH and RV failure.

ARTICLE INFORMATION

Received October 8, 2019; accepted December 28, 2020.

Affiliations

Department of Cardiovascular Medicine, Tohoku University Graduate School of Medicine, Sendai, Japan.

Acknowledgments

We are grateful to the laboratory members in the Department of Cardiovascular Medicine at Tohoku University for valuable technical assistance, especially Yumi Watanabe, Ai Nishihara, and Hiromi Yamashita.

Sources of Funding

This work was supported in part by the grants-in-aid for Scientific Research (15H02535, 15H04816, and 15K15046), all of which are from the Ministry of Education, Culture, Sports, Science and Technology, Tokyo, Japan, the grants-in-aid for Scientific Research from the Ministry of Health, Labour, and Welfare, Tokyo, Japan (10102895), and the grants-in-aid for Scientific Research from the Japan Agency for Medical Research and Development, Tokyo, Japan (15ak0101035h0001, 16ek0109176h0001, 17ek0109227h0001).

Disclosures

None.

REFERENCES

1. Ryan JJ, Archer SL. Emerging concepts in the molecular basis of pulmonary arterial hypertension: part I: metabolic plasticity and mitochondrial dynamics in the pulmonary circulation and right ventricle in pulmonary arterial hypertension. *Circulation*. 2015;131:1691–1702. doi: 10.1161/CIRCULATIONAHA.114.006979
2. Kurosawa R, Satoh K, Kikuchi N, Kikuchi H, Saigusa D, Al-Mamun ME, Siddique MAH, Omura J, Satoh T, Sunamura S, et al. Identification of celastramycin as a novel therapeutic agent for pulmonary arterial hypertension. *Circ Res*. 2019;125:309–327. doi: 10.1161/CIRCRESAHA.119.315229
3. Omura J, Satoh K, Kikuchi N, Satoh T, Kurosawa R, Nogi M, Ohtsuki T, Al-Mamun ME, Siddique MAH, Yaoita N, et al. ADAMTS8 promotes the development of pulmonary arterial hypertension and right ventricular failure: a possible novel therapeutic target. *Circ Res*. 2019;125:884–906. doi: 10.1161/CIRCRESAHA.119.315398
4. Siddique MAH, Satoh K, Kurosawa R, Kikuchi N, Elias-Al-Mamun M, Omura J, Satoh T, Nogi M, Sunamura S, Miyata S, et al. Identification of emetine as a therapeutic agent for pulmonary arterial hypertension: novel effects of an old drug. *Arterioscler Thromb Vasc Biol*. 2019;39:2367–2385. doi: 10.1161/ATVBAHA.119.313309
5. Kikuchi N, Satoh K, Kurosawa R, Yaoita N, Elias-Al-Mamun M, Siddique MAH, Omura J, Satoh T, Nogi M, Sunamura S, et al. Selenoprotein P promotes the development of pulmonary arterial hypertension: possible novel therapeutic target. *Circulation*. 2018;138:600–623. doi: 10.1161/CIRCULATIONAHA.117.033113
6. Kikuchi N, Satoh K, Satoh T, Yaoita N, Siddique MAH, Omura J, Kurosawa R, Nogi M, Sunamura S, Miyata S, et al. Diagnostic and prognostic significance of serum levels of SeP (Selenoprotein P) in patients with pulmonary hypertension. *Arterioscler Thromb Vasc Biol*. 2019;39:2553–2562. doi: 10.1161/ATVBAHA.119.313267
7. Miura Y, Fukumoto Y, Sugimura K, Oikawa M, Nakano M, Tatebe S, Miyamichi S, Satoh K, Shimokawa H. Identification of new prognostic factors of pulmonary hypertension. *Circ J*. 2010;74:1965–1971. doi: 10.1253/circj.cj-10-0270
8. Elias-Al-Mamun M, Satoh K, Tanaka S-I, Shimizu T, Nergui S, Miyata S, Fukumoto Y, Shimokawa H. Combination therapy with fasudil and sildenafil ameliorates monocrotaline-induced pulmonary hypertension and survival in rats. *Circ J*. 2014;78:967–976. doi: 10.1253/circj.cj-13-1174
9. Shimokawa H, Satoh K. 2015 ATVB Plenary Lecture: translational research on rho-kinase in cardiovascular medicine. *Arterioscler Thromb Vasc Biol*. 2015;35:1756–1769. doi: 10.1161/ATVBAHA.115.305353
10. Kina-Tanada M, Sakanashi M, Tanimoto A, Kaname T, Matsuzaki T, Noguchi K, Uchida T, Nakasone J, Kozuka C, Ishida M, et al. Long-term dietary nitrite and nitrate deficiency causes the metabolic syndrome, endothelial dysfunction and cardiovascular death in mice. *Diabetologia*. 2017;60:1138–1151. doi: 10.1007/s00125-017-4259-6
11. Yaoita N, Shirakawa R, Fukumoto Y, Sugimura K, Miyata S, Miura Y, Nochioka K, Miura M, Tatebe S, Aoki T, et al. Platelets are highly activated in patients of chronic thromboembolic pulmonary hypertension. *Arterioscler Thromb Vasc Biol*. 2014;34:2486–2494. doi: 10.1161/ATVBAHA.114.304404
12. Satoh T, Satoh K, Yaoita N, Kikuchi N, Omura J, Kurosawa R, Numano K, Al-Mamun E, Siddique MA, Sunamura S, et al. Activated TAFI promotes the development of chronic thromboembolic pulmonary hypertension: a possible novel therapeutic target. *Circ Res*. 2017;120:1246–1262. doi: 10.1161/CIRCRESAHA.117.310640
13. Iacono KT, Brown AL, Greene MI, Saouaf SJ.. CD147 immunoglobulin superfamily receptor function and role in pathology. *Exp Mol Pahol*. 2007;83:283–295. doi: 10.1016/j.yexmp.2007.08.014
14. Satoh K, Satoh T, Kikuchi N, Omura J, Kurosawa R, Suzuki K, Sugimura K, Aoki T, Nochioka K, Tatebe S, et al. Basigin mediates pulmonary hypertension by promoting inflammation and vascular smooth muscle cell proliferation. *Circ Res*. 2014;115:738–750. doi: 10.1161/CIRCRESAHA.115.304563
15. Suzuki K, Satoh K, Ikeda S, Sunamura S, Otsuki T, Satoh T, Kikuchi N, Omura J, Kurosawa R, Nogi M, et al. Basigin promotes cardiac fibrosis and

Downloaded from http://ahajournals.org by on March 22, 2021

failure in response to chronic pressure overload in mice. *Arterioscler Thromb Vasc Biol.* 2016;36:636–646. doi: 10.1161/ATVBAHA.115.306686
16. Ke H, Huai Q. Ctystal structures of cyclophilin and its partners. *Front Biosci.* 2004;9:2285–2296. doi: 10.2741/1396
17. Satoh K, Godo S, Saito H, Enkhjargal B, Shimokawa H. Dual roles of vascular-derived reactive oxygen species–with a special reference to hydrogen peroxide and cyclophilin A. *J Mol Cell Cardiol.* 2014;73:50–56. doi: 10.1016/j.yjmcc.2013.12.022
18. Satoh K. Cyclophilin A in cardiovascular homeostasis and diseases. *Tohoku J Exp Med.* 2015;235:1–15. doi: 10.1620/tjem.235.1
19. Satoh K, Nigro P, Matoba T, O'Dell MR, Cui Z, Shi X, Mohan A, Yan C, Abe J, Illig KA, et al. Cyclophilin A enhances vascular oxidative stress and the development of angiotensin II-induced aortic aneurysms. *Nat Med.* 2009;15:649–656. doi: 10.1038/nm.1958
20. Satoh K, Nigro P, Zeidan A, Soe NN, Jaffré F, Oikawa M, O'Dell MR, Cui Z, Menon P, Lu Y, et al. Cyclophilin A promotes cardiac hypertrophy in apolipoprotein E-deficient mice. *Arterioscler Thromb Vasc Biol.* 2011;31:1116–1123. doi: 10.1161/ATVBAHA.110.214601
21. Sunamura S, Satoh K, Kurosawa R, Ohtsuki T, Kikuchi N, Elias-Al-Mamun M, Shimizu T, Ikeda S, Suzuki K, Satoh T, et al. Different roles of myocardial ROCK1 and ROCK2 in cardiac dysfunction and postcapillary pulmonary hypertension in mice. *Proc Natl Acad Sci U S A.* 2018;115:E7129–E7138. doi: 10.1073/pnas.1721298115
22. Tatebe S, Fukumoto Y, Sugimura K, Miyamichi-Yamamoto S, Aoki T, Miura Y, Nochioka K, Satoh K, Shimokawa H. Clinical significance of reactive postcapillary pulmonary hypertension in patients with left heart disease. *Circ J.* 2012;76:1235–1244. doi: 10.1253/circj.cj-11-1288
23. Li MP, Hu XL, Yang YL, Zhang YJ, Zhou JP, Peng LM, Tang J, Chen XP. Basigin rs8259 polymorphism confers decreased risk of chronic heart failure in a Chinese population. *Int J Environ Res Public Health.* 2017;14:211. doi: 10.3390/ijerph14020211
24. Yan J, Mao Y, Wang C, Wang Z. Association Study between an SNP in CD147 and its expression with acute coronary syndrome in a Jiangsu Chinese population. *Medicine (Baltimore).* 2015;94:e1537. doi: 10.1097/MD.0000000000001537
25. Cascão R, Fonseca JE, Moita LF. Celastrol: a spectrum of treatment opportunities in chronic diseases. *Front Med (Lausanne).* 2017;4:69. doi: 10.3389/fmed.2017.00069
26. Yurchenko V, Constant S, Eisenmesser E, Bukrinsky M. Cyclophilin-CD147 interactions: a new target for anti-inflammatory therapeutics. *Clin Exp Immunol.* 2010;160:305–317. doi: 10.1111/j.1365-2249.2010.04115.x
27. Zhu D, Wang Z, Zhao JJ, Calimeri T, Meng J, Hideshima T, Fulciniti M, Kang Y, Ficarro SB, Tai YT, et al. The cyclophilin A-CD147 complex promotes the proliferation and homing of multiple myeloma cells. *Nat Med.* 2015;21:572–580. doi: 10.1038/nm.3867
28. Seizer P, Ochmann C, Schönberger T, Zach S, Rose M, Borst O, Klingel K, Kandolf R, MacDonald HR, Nowak RA, et al. Disrupting the EMMPRIN (CD147)-cyclophilin A interaction reduces infarct size and preserves systolic function after myocardial ischemia and reperfusion. *Arterioscler Thromb Vasc Biol.* 2011;31:1377–1386. doi: 10.1161/ATVBAHA.111.225771
29. Spinale FG, Coker ML, Heung LJ, Bond BR, Gunasinghe HR, Etoh T, Goldberg AT, Zellner JL, Crumbley AJ. A matrix metalloproteinase induction/activation system exists in the human left ventricular myocardium and is upregulated in heart failure. *Circulation.* 2000;102:1944–1949. doi: 10.1161/01.cir.102.16.1944
30. Seizer P, Geisler T, Bigalke B, Schneider M, Klingel K, Kandolf R, Stellos K, Schreieck J, Gawaz M, May AE. EMMPRIN and its ligand cyclophilin A as novel diagnostic markers in inflammatory cardiomyopathy. *Int J Cardiol.* 2013;163:299–304. doi: 10.1016/j.ijcard.2011.06.049
31. Abe K, Toba M, Alzoubi A, Ito M, Fagan KA, Cool CD, Voelkel NF, McMurtry IF, Oka M. Formation of plexiform lesions in experimental severe pulmonary arterial hypertension. *Circulation.* 2010;121:2747–2754. doi: 10.1161/CIRCULATIONAHA.109.927681
32. Simpson P. Stimulation of hypertrophy of cultured neonatal rat heart cells through an alpha 1-adrenergic receptor and induction of beating through an alpha 1- and beta 1-adrenergic receptor interaction. Evidence for independent regulation of growth and beating. *Circ Res.* 1985;56:884–894. doi: 10.1161/01.res.56.6.884
33. Zavadzkas JA, Plyler RA, Bouges S, Koval CN, Rivers WT, Beck CU, Chang EI, Stroud RE, Mukherjee R, Spinale FG. Cardiac-restricted overexpression of extracellular matrix metalloproteinase inducer causes myocardial remodeling and dysfunction in aging mice. *Am J Physiol Heart Circ Physiol.* 2008;295:H1394–H1402. doi: 10.1152/ajpheart.00346.2008
34. Siwik DA, Kuster GM, Brahmbhatt JV, Zaidi Z, Malik J, Ooi H, Ghorayeb G. EMMPRIN mediates beta-adrenergic receptor-stimulated matrix metalloproteinase activity in cardiac myocytes. *J Mol Cell Cardiol.* 2008;44:210–217. doi: 10.1016/j.yjmcc.2007.07.054
35. Liu J, Lee J, Salazar Hernandez MA, Mazitschek R, Ozcan U. Treatment of obesity with celastrol. *Cell.* 2015;161:999–1011. doi: 10.1016/j.cell.2015.05.011
36. Tang Y, Kesavan P, Nakada MT, Yan L. Tumor-stroma interaction: positive feedback regulation of extracellular matrix metalloproteinase inducer (EMMPRIN) expression and matrix metalloproteinase-dependent generation of soluble EMMPRIN. *Mol Cancer Res.* 2004;2:73–80.
37. Okada M, Kikuzuki R, Harada T, Hori Y, Yamawaki H, Hara Y. Captopril attenuates matrix metalloproteinase-2 and -9 in monocrotaline-induced right ventricular hypertrophy in rats. *J Pharmacol Sci.* 2008;108:487–494. doi: 10.1254/jphs.08174fp
38. Lu G, Jia Z, Zu Q, Zhang J, Zhao L, Shi H. Inhibition of the cyclophilin A-CD147 interaction attenuates right ventricular injury and dysfunction after acute pulmonary embolism in rats. *J Biol Chem.* 2018;293:12199–12208. doi: 10.1074/jbc.RA118.002845
39. Hong F, Lee J, Piao YJ, Jae YK, Kim YJ, Oh C, Seo JS, Yun YS, Yang CW, Ha J, et al. Transgenic mice overexpressing cyclophilin A are resistant to cyclosporin A-induced nephrotoxicity via peptidyl-prolyl cis-trans isomerase activity. *Biochem Biophys Res Commun.* 2004;316:1073–1080. doi: 10.1016/j.bbrc.2004.02.160
40. Huang Z, Wang L, Meng S, Wang Y, Chen T, Wang C. Berberine reduces both MMP-9 and EMMPRIN expression through prevention of p38 pathway activation in PMA-induced macrophages. *Int J Cardiol.* 2011;146:153–158. doi: 10.1016/j.ijcard.2009.06.023
41. Huang Z, Wang C, Wei L, Wang J, Fan Y, Wang L, Wang Y, Chen T. Resveratrol inhibits EMMPRIN expression via P38 and ERK1/2 pathways in PMA-induced THP-1 cells. *Biochem Biophys Res Commun.* 2008;374:517–521. doi: 10.1016/j.bbrc.2008.07.058
42. Cao J, Han Z, Tian L, Chen K, Fan Y, Ye B, Huang W, Wang C, Huang Z. Curcumin inhibits EMMPRIN and MMP-9 expression through AMPK-MAPK and PKC signaling in PMA induced macrophages. *J Transl Med.* 2014;12:266. doi: 10.1186/s12967-014-0266-2
43. Damsker JM, Okwumabua I, Pushkarsky T, Arora K, Bukrinsky MI, Constant SL. Targeting the chemotactic function of CD147 reduces collagen-induced arthritis. *Immunology.* 2009;126:55–62. doi: 10.1111/j.1365-2567.2008.02877.x
44. Macmillan ML, Couriel D, Weisdorf DJ, Schwab G, Havrilla N, Fleming TR, Huang S, Roskos L, Slavin S, Shadduck RK, et al. A phase 2/3 multicenter randomized clinical trial of ABX-CBL versus ATG as secondary therapy for steroid-resistant acute graft-versus-host disease. *Blood.* 2007;109:2657–2662. doi: 10.1182/blood-2006-08-013995
45. Zhu P, Lu N, Shi ZG, Zhou J, Wu ZB, Yang Y, Ding J, Chen ZN. CD147 overexpression on synoviocytes in rheumatoid arthritis enhances matrix metalloproteinase production and invasiveness of synoviocytes. *Arthritis Res Ther.* 2006;8:R44. doi: 10.1186/ar1899
46. Chen X, Lin J, Kanekura T, Su J, Lin W, Xie H, Wu Y, Li J, Chen M, Chang J. A small interfering CD147-targeting RNA inhibited the proliferation, invasiveness, and metastatic activity of malignant melanoma. *Cancer Res.* 2006;66:11323–11330. doi: 10.1158/0008-5472.CAN-06-1536
47. Arora K, Gwinn WM, Bower MA, Watson A, Okwumabua I, MacDonald HR, Bukrinsky MI, Constant SL. Extracellular cyclophilins contribute to the regulation of inflammatory responses. *J Immunol.* 2005;175:517–522. doi: 10.4049/jimmunol.175.1.517
48. Pinna GF, Fiorucci M, Reimund JM, Taquet N, Arondel Y, Muller CD. Celastrol inhibits pro-inflammatory cytokine secretion in Crohn's disease biopsies. *Biochem Biophys Res Commun.* 2004;322:778–786. doi: 10.1016/j.bbrc.2004.07.186
49. Kim DY, Park JW, Jeoung D, Ro JY. Celastrol suppresses allergen-induced airway inflammation in a mouse allergic asthma model. *Eur J Pharmacol.* 2009;612:98–105. doi: 10.1016/j.ejphar.2009.03.078
50. Bakar MH, Sarmidi MR, Kai CK, Huri HZ, Yaakob H. Amelioration of mitochondrial dysfunction-induced insulin resistance in differentiated 3T3-L1 adipocytes via inhibition of NF-κB pathways. *Int J Mol Sci.* 2014;15:22227–22257. doi: 10.3390/ijms151222227
51. Wang C, Jin R, Zhu X, Yan J, Li G. Function of CD147 in atherosclerosis and atherothrombosis. *J Cardiovasc Transl Res.* 2015;8:59–66. doi: 10.1007/s12265-015-9608-6
52. Schmidt R, Bültmann A, Fischel S, Gillitzer A, Cullen P, Walch A, Jost P, Ungerer M, Tolley ND, Lindemann S, et al. Extracellular matrix metalloproteinase inducer (CD147) is a novel receptor on platelets, activates platelets, and augments nuclear factor kappaB-dependent inflammation in monocytes. *Circ Res.* 2008;102:302–309. doi: 10.1161/CIRCRESAHA.107.157990

Downloaded from http://ahajournals.org by on March 22, 2021